

IN SEARCH OF PREBASIN HIGHLANDS COMPONENTS AND TYCHO EJECTA IN APOLLO 17 DRIVE TUBE 73002 USING CONTINUOUS CORE SECTION QUANTITATIVE ANALYSIS. B. L. Jolliff^{1,3}, P. K. Carpenter^{1,3}, C. J.-K. Yen^{1,3}, M. D. Neuman^{1,3}, R. C. Ogliore^{2,3}, A. Minocha^{2,3}, and the ANGSA Science Team⁴, ¹Department of Earth & Planetary Sciences, ²Department of Physics, ³The McDonnell Center for the Space Sciences, Washington University in St. Louis, MO 63130, and ⁴www.lpi.usra.edu/ANGSA/teams/, (bjolliff@wustl.edu).

Introduction: The Apollo 17 massif deposits offer a glimpse into the pre-basin crust of the Moon in the Taurus Littrow region. The massif regolith as sampled at Apollo 17 contains a wide variety of components, known from large-rock samples, including several compositional and textural varieties of mafic impact-melt breccia (poikilitic, aphanitic, incompatible-element rich [1,2] as well as more anorthositic, incompatible-element poor lithologies. Korotev and Kremser [3] and Korotev [4] considered a range of compositional components in their analysis of Apollo 17 soils. They defined the prominent nonmare compositional components as “noritic breccia” – the mafic impact melt that composes, for example, the large boulders sampled on North Massif, and “anorthositic norite” or AN – which represents a variety of materials including granulitic breccias and other incompatible-element-poor lithologies. Because they lack mare components and incompatible-element-rich impact-melt components, these lithologies may represent the prebasin highlands of the Moon and, accordingly, are significantly poorer in FeO (e.g., 3-7 wt.%) compared to mafic impact-melt breccia (8-10 wt.%). Neuman et al. [5] model the composition of the 73002 drive tube <1 mm soil intervals in terms of these and several mare lithologic components, and find that the AN component is the major compositional component, making up ~50-60 wt.% of the soil. Here, we investigate the continuous core thin sections for non-mare glass and lithic fragment compositions that might represent these AN components. Among the incompatible-

element-poor, low-FeO-composition materials we anticipate possibly finding a new candidate for Tycho impact melt, expected from remote sensing to be FeO-poor and of gabbroic anorthosite composition (see below).

Samples and Methods: Double drive tube 73001/2 was collected at station 3, located on the light mantle deposit at the base of South Massif [6]. The light-mantle deposit is much less contaminated with mare material than other nonmare Apollo 17 stations such as those at the base of North massif [3] and thus offers an opportunity to search for these ancient pre-basin components. In this work, we use the 73002 continuous core thin sections and quantitative EPMA mapping as described by [7,8]. We retrieved the bulk compositions of a range of glasses, vitrophyres, and very fine grained impact melt and impact-melt breccia matrices, using the Q-tool [8]. Examples are shown in Fig. 1. We retrieved compositions with oxide sums ranging from 97 to 101 wt.% for 45 clasts in four thin sections, 73002,6015-6018. We selected specifically for nonmare compositions and sought a range of component compositions that represent different nonmare lithologic components for

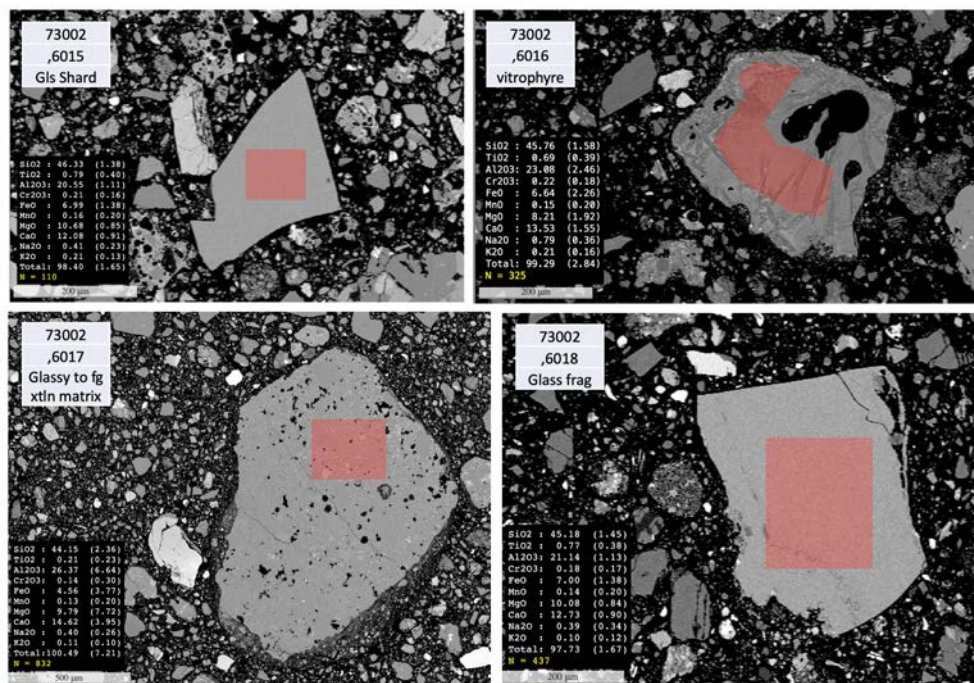


Figure 1. Examples of clasts in continuous core thin sections with compositional retrieval areas indicated by pink regions. All four represent relatively feldspathic compositions that contribute to the anorthositic norite component composition. Backscattered electron images. Scale bars in lower left of frame.

comparison. These included glass compositions representing local regolith (glass fragments and agglutinitic glass), impact-melt components representing mafic impact-melt breccias, and FeO-poor, feldspathic compositions that potentially represent prebasin upper crustal materials, possibly including Tycho impact-melt components. Each composition represents an average of between 25 and 15,000 pixels (quantitative X-ray spot analyses [7] and clast sizes range from ~80 μm to >1 mm).

Results and Discussion: In our data retrieval, we avoided mare lithic fragments and volcanic glasses, and single mineral clasts or coarsely crystalline materials. The dataset is not intended to reflect relative proportions of different compositions, but instead to reflect specific components. Compositional plots such as FeO vs. TiO_2 (Fig. 2) define several distinct clusters of compositions. Mafic impact-melt breccias plot in the range of ~8-10 wt.% FeO and around 2 wt.% TiO_2 . All of the ones in our selected set have aphanitic matrix.

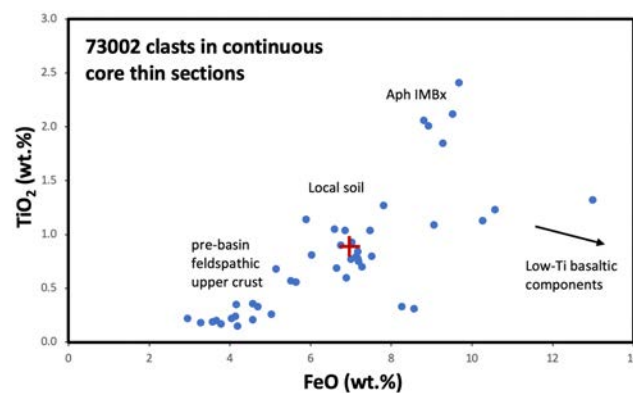


Figure 2. Select set of compositions of relatively homogeneous composition clasts in continuous core thin sections, including agglutinate glass, glass fragments, vitrophyres, fine-grained impact melt, and aphanitic impact-melt breccia matrix. Red cross represents the composition of regolith breccia/soil clod 73131.

Numerous compositions lie in the range 6-8 wt.% FeO and 0.5-1.2 wt.% TiO_2 . These compositions cluster around the composition of Station 2A regolith clod 73131 [3], which we take to be an approximation of the mare-free composition of the regolith prior to emplacement of the light mantle [3].

A third group has FeO values <6 wt.% and TiO_2 <0.6 wt.%. These materials may represent regolith and lithologic components formed prior to admixture with either mare components or impact-melt breccias that are characterized by enrichment in incompatible lithophile trace elements. We presume that the mafic impact-melt breccias derive from Serenitatis basin or possibly some other basin [9], thus the lithic components lacking these would represent pre-basin materials.

Tycho Component? Compositional remote sensing data for FeO, TiO_2 , and thorium [10-12] indicate that Tycho struck the lunar crust in a region of low FeO (3-4 wt.%), low TiO_2 , (<1 wt.%), and low thorium, thus KREEP-poor. Mineralogic remote sensing [13] suggests a gabbroic anorthosite composition, with ~80% plagioclase and a relatively high clinopyroxene content, e.g., 7-12%. Most of the compositions we encounter among the 73002 clast compositions are more noritic in composition (orthopyroxene > clinopyroxene in the norm). However, we do find glassy components with such low FeO and TiO_2 , and with very low incompatible element contents, judging by measured K_2O (~0.1 or less wt.% K_2O).

The data in this abstract serve as an example of the kind of high-quality compositional information contained in the quantitative EPMA (WDS) mapping and powerful data retrieval with the Q-tool that can be harnessed to search for candidate materials not only of the pre-basin highlands but perhaps also of Tycho origin.

Further work: The data thus collected from the 73002 core continuous thin sections represent a “next generation” capability that enables many researchers to interrogate the data in a preliminary – or rigorous – way, depending on their specific objective, and to request sections for further analysis accordingly. Fruitful avenues for research include the study of glasses, agglutinates, and lithic fragments of a variety of rock types and mineral assemblages.

Acknowledgments: We thank the curatorial staff at JSC and the preliminary examination (PE) team for their work in dissecting and preparing the core samples. We appreciate the excellent work of Jeremy Kent in preparing the continuous thin sections and for the transmitted- and reflected-light photomicrographs. We thank NASA for supporting the ANGSA project.

References: [1] Spudis and Ryder (1981) *PLPSC* **12A**, 133-148. [2] Jolliff et al. (1996) *MAPS* **31**, 116-145 **180**, 1052-1055. [3] Korotev and Kremser (1992) *PLPSC* **22**, 275-301. [4] Korotev (2022) *MAPS* **8**, in press. [5] Neuman et al. (2022) *This Workshop*. [6] Wolfe et al. (1981) USGS Prof. Paper **1080**:280 [7] Carpenter et al. (2022) *This Workshop*. [8] Minocha et al. (2022) *This Workshop*. [9] Spudis et al. (2011) *JGR-P* **116**, E00H03. [10] Lawrence et al. (2000) *JGR-P* **105**, 20307-20331. [11] Lawrence et al. (2002) *JGR-P* **107**, 5130. [12] Sato et al. (2017) *Icarus* **296**, 216-238. [13] Lemelin et al. (2019) *PSS* **165**, 230-243.